Investigation on the formation of tungsten carbide in tungsten-containing diamond like carbon coatings

Strondl, C.; Carvalho, N.M.; Hosson, J.Th.M. De; Kolk, G.J. van der

Link to publication in University of Groningen/UMCG research database

Investigation on the formation of tungsten carbide in tungsten-containing diamond like carbon coatings

C. Strondl[a],*, N.M. Carvalho[b], J.Th.M. De Hosson[b], G.J. van der Kolk[a]

[a]*Hauzer Techno Coating BV, van Heemskerckweg 22, NL-5928 LL Venlo, The Netherlands*
[b]*Department of Applied Physics, Material Science Centre and Netherlands Institute of Metals Research, University of Groningen, Nijenborgh 4,
NL-9747 AG Groningen, The Netherlands*

Abstract

A series of tungsten-containing diamond-like carbon (Me-DLC) coatings have been produced by unbalanced magnetron sputtering using a Hauzer HTC-1000 production PVD system. Sputtering from WC targets has been used to form W-C:H coatings. The metal to carbon ratio has been varied to study changes in the metal carbide formation and distribution within the amorphous hydrocarbons (a-C:H) matrix. The difference in the formation of the metal carbide is then linked to changes in the mechanical and tribological properties of the coatings. Detailed high-resolution cross-section TEM has been carried out to analyze the microstructure of the coatings. By changing the amount of a-C:H in the W-C:H coatings, the coefficient of friction could be varied between 0.129 and 0.312. The hardness was found to vary between 8 and 27.5 GPa by using different acetylene gas flows. It was observed that all coatings did have a pronounced multilayered structure.
© 2002 Elsevier Science B.V. All rights reserved.

1. Introduction

A series of tungsten containing diamond like carbon (Me-DLC) coatings generally have a low coefficient of friction in combination with a high wear resistance [1]. Even, if many properties between Me-DLC coatings and pure DLC coating are similar, there are some fundamental differences between the two types of coatings. Me-DLC is recognized as having lower intrinsic compressive stress compared to pure DLC coatings [2,3]. This stress level results in a markedly better adhesion of the Me-DLC coatings onto steel substrates. The high adhesion level of Me-DLC coatings is the main reason why these coatings are successfully used in many industrial applications [4–7].

In this paper, W-C:H coatings with varying metal to carbon ratio have been deposited. The investigation is aimed at examining the difference in microstructure between the different coatings and at making a linkage to mechanical and tribological properties like hardness and coefficient of friction.

2. Experimental details

2.1. Deposition

Four different W-C:H coatings have been deposited with unbalanced magnetron sputtering in an argon/acetylene atmosphere in a Hauzer HTC-1000 production scale coating system. The metal content in the Me-DLC coating is determined by sputtering of WC targets. The Hauzer HTC-1000 coating system uses a system of electromagnetic coils to control the degree of unbalancing of the magnetic field of the sputtering cathodes. The effect of unbalancing the magnetic field makes it possible to control the degree of plasma density around the substrates and, in case of Me-DLC deposition, this in turn determines the plasma-assisted CVD (PA-CVD) from the hydrocarbon gas phase. All cathodes have individual shutters to be able to clean the targets with

*Corresponding author.
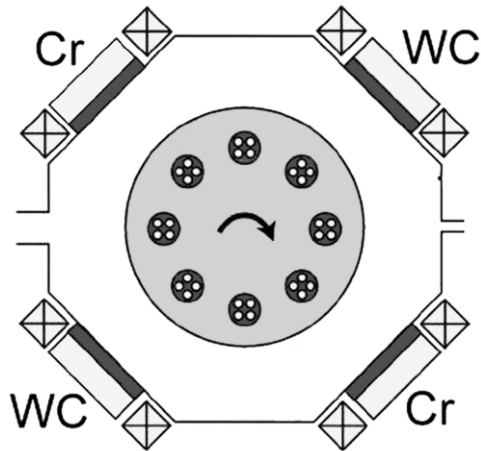E-mail address:* cstrondl@hauzer.nl (C. Strondl).

Fig. 1. Set-up of Hauzer HTC-1000 production coating system.

sputtering before deposition and to protect the target surface from cross-contamination when not in use. Two rotating thermocouples mounted directly on the rotating substrate table were used to accurately control the temperature of the substrates during deposition. This is particularly important when coating heat sensitive steel substrates like 100Cr6 (DIN1.3505, SAE 52100).

The set-up of the Hauzer HTC-1000 coating system was with two Cr targets and two WC targets opposing each other (Fig. 1). The Cr targets were used to create an interface layer between the W-C:H coating and the substrate material.

Flat HSS (HRc 60–62) and stainless steel test pieces polished to a surface roughness of $R_a < 60$ nm were used for the different coatings. All test pieces were deposited with a twofold planetary rotation.

Four different coatings (named: 25, 50, 100 and 140 sccm) deposited with different flow of acetylene were investigated, see Table 1 for details about the process parameters.

2.2. Evaluation techniques

The coefficient of friction was measured with a CSEM tribometer pin-on-disc (Al_2O_3 ball with 6 mm diameter, 0.010 m/s, 15000 revolutions, 22 mm track diameter, 5 N load). A CSEM Revetest scratch tester was used for measuring the adhesion (200 μm radius on stylus, 0.001

m/s, and a constant load). The surface roughness was measured with an AFM (Digital Instruments Dimension 3100) apparatus. The surface characterization was carried out in tapping mode to avoid any damage to the film surface. The radius of the cantilever tip was $\leqslant 10$ nm with a side angle $\leqslant 10°$. The hardness and Young's modulus of the coatings were measured with a fully calibrated MTS Nano Indenter® XP. The indenter used was of Berkovich type. The instrument operates in load control mode and is equipped with a continuous stiffness measurement (CSM) module and a high load cell. The CSM option allows the contact stiffness to be measured continuously during the loading portion of the test, differing from the conventional load–displacement–time method where only one contact stiffness measurement is made from the unloading portion of the experiment at P_{max}. For the experiments performed in this study, the CSM imposed a 1 nm oscillation at 45 Hz on the loading curve. The indentation system and contact together are modeled as a simple harmonic oscillator. Thus, by monitoring the ratio between force and displacement oscillation amplitudes, as well as phase shift between the two, the elastic stiffness of the contact may be inferred continuously as the indenter penetrates the material. A standard approach-load–unload cycle was used, where the load was held at full load and at 70% of maximum load on unloading to allow for compensation of creep and calculation of any thermal drift effects, respectively. The raw data were then processed to correct for thermal drift, load-frame compliance, and to produce load–displacement (P–δ) curves. The measurements were repeated 20 times and were all loaded such that the loading rate divided by the load was held constant at 0.05 s^{-1}. This procedure permits a large number of data points to be accumulated in the low-load segment. This is particularly useful when undertaking experiments on coated systems. The standard deviation was used as a measure of the experimental accuracy.

The stress measurements were carried out on 4 in. Si wafer substrates. The Si wafer curvature was measured by the principle of distance deviation of two reflected parallel laser beams before and after the deposition step and was used for calculating the biaxial stress in the coatings [8,9].

The coating morphology was examined using scanning electron microscopy (Philips FEG-XL30) on pol-

Table 1
Process parameters for investigated coatings

Sample name	25 sccm	50 sccm	100 sccm	140 sccm
Target material	WC			
Target power	2×5 kW			
Sputter pressure	∼0.3 Pa			
Gas flow C_2H_2	25 sccm	50 sccm	100 sccm	140 sccm
Substrate table rotation speed	0.5 rpm			

Table 2
Measured coating thickness, adhesion, coefficient of friction and surface roughness

Sample name	25 sccm	50 sccm	100 sccm	140 sccm
Coating thickness (μm)	2.15	2.16	2.52	2.43
Adhesion (critical load)	$\geqslant 50$ N			
Coefficient of friction	0.312	0.290	0.163	0.129
Initial surface roughness substrate (R_a) (μm)	0.06	0.06	0.06	0.05
Surface roughness after deposition (R_a) (μm)	0.08	0.07	0.06	0.05

ished samples. The investigation of the micro structure was carried out by transmission electron microscopy (JEOL 4000 EX/II), operating at 400 kV with a spherical aberration constant $C_s = 0.97$ mm and wavelength of $\lambda = 1.64$ pm.

3. Results and discussion

3.1. Coating thickness, adhesion and coefficient of friction

The coating thickness, adhesion and coefficient of friction are summarized in Table 2. It can be seen that the coefficient of friction is inversely proportional to the flow of acetylene. With increasing flow of acetylene, the amount of amorphous hydrocarbons (a-C:H) in the coating is increasing [10]. This most likely results in an easier graphitization process of the coating and an easier formation of the transfer layer during sliding contact, and thus a lower coefficient of friction in the pin-on-disc test. All the different coatings vary in thickness between 2.15 and 2.52 μm. The adhesion measurements with scratch testing show that all coatings have good adhesion levels ($\geqslant 50$ N critical load).

3.2. Surface roughness

A small difference in surface roughness (R_a) could be detected between the coatings (Table 2). At low flows of acetylene, the R_a value increases slightly compared to the original uncoated surface roughness of the substrate. With higher flows of acetylene, the coatings are very smooth and no increase in R_a value from the initial substrate roughness could be measured.

3.3. Nano-indentation

In Figs. 2 and 3 the nano-indentation results are presented. A very clear difference in hardness and E-modulus can be seen between the coatings with different acetylene flows. The hardest coating was the one of 25 sccm acetylene flow with a measured peak hardness of approximately 27.5 GPa. The second hardest coating was 50 sccm acetylene with a peak hardness of approximately 18 GPa, followed by the 100 sccm acetylene with a peak hardness of approximately 12.5 GPa. The softest of the four coatings was the 140 sccm acetylene with a hardness of approximately 8 GPa. The E-modulus for the four different coatings follows the same trend as for the hardness. At the point of peak hardness, the corresponding E-modulus for the sample with 25 sccm
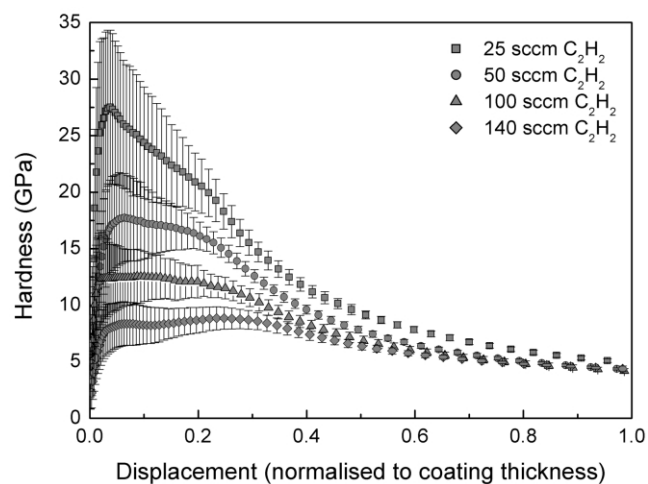

Fig. 2. Hardness measurement with nano-indentation technique as a function of coating depth for the W-C:H coatings.
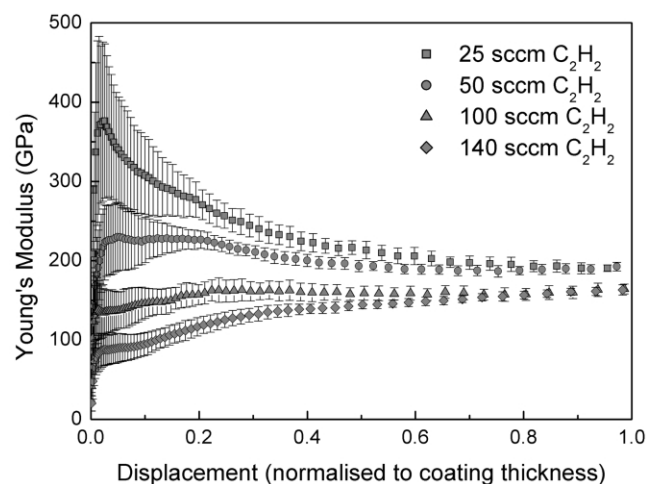

Fig. 3. E-modulus measurement with nano-indentation technique as a function of coating depth for the W-C:H coatings.
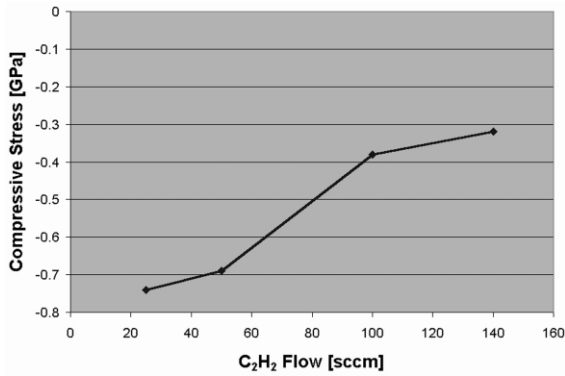
Fig. 4. Stress measurement on the W-C:H coatings carried out with the bending method on Si wafers.

acetylene is approximately 380 GPa. For the sample with 50 sccm acetylene the corresponding E-modulus was approximately 230 GPa and for the 100 sccm acetylene approximately 140–150 GPa. The softest coating with 140 sccm acetylene had a corresponding E-modulus of approximately 90–100 GPa. It is clear from the nano-indentation measurements that it is the ratio between the hard WC and the softer a-C:H that controls the hardness of the W-C:H system in this investigation. The process conditions for the W-C:H coatings are such

that it results in a very soft a-C:H matrix and the higher the ratio of a-C:H to WC is, the softer the W-C:H coatings become. High amount of WC in the a-C:H matrix results thus in a harder coating.

3.4. Stress measurement

The stress measurements are presented in Fig. 4. The highest compressive stress level was measured to be −0.74 GPa for the coating with 25 sccm acetylene flow. The coating with 50 sccm acetylene had a compressive stress level of −0.69 GPa, followed by the 100 sccm acetylene with −0.38 GPa and 140 sccm acetylene with −0.32 GPa. A clear trend can be seen in the compressive stress level. Higher acetylene flow, which corresponds to a higher amount of a-C:H in the W-C:H coatings, show a lower compressive stress level and the coatings with a lower acetylene flow, which corresponds to a lower amount of a-C:H in the W-C:H coatings, show a higher compressive stress.

3.5. Cross-section SEM and TEM

The morphology of the coatings can be seen in the cross-sectional SEM micrographs in Fig. 5a–d. A pronounced multilayered coating structure with alternating
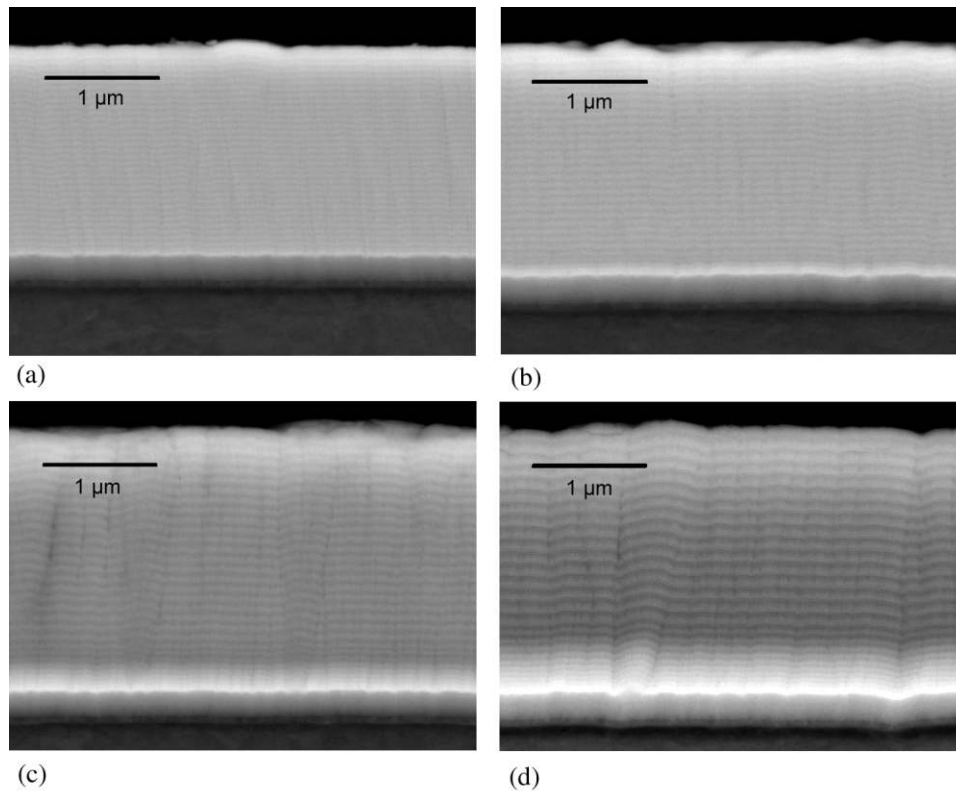

Fig. 5. Microstructure of polished cross-section SEM in BSE mode from (a) 25 sccm; (b) 50 sccm; (c) 100 sccm and (d) 140 sccm acetylene flow.
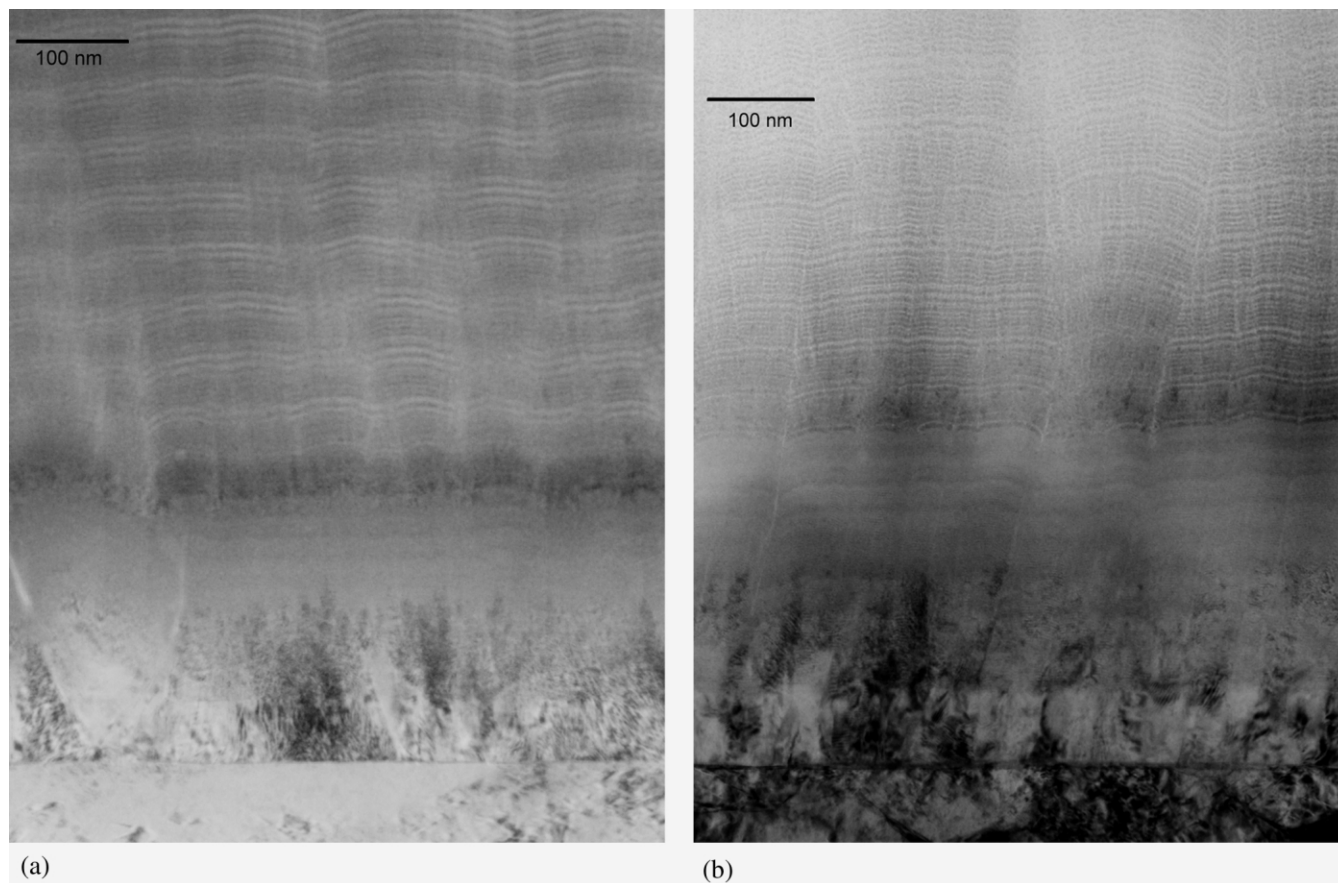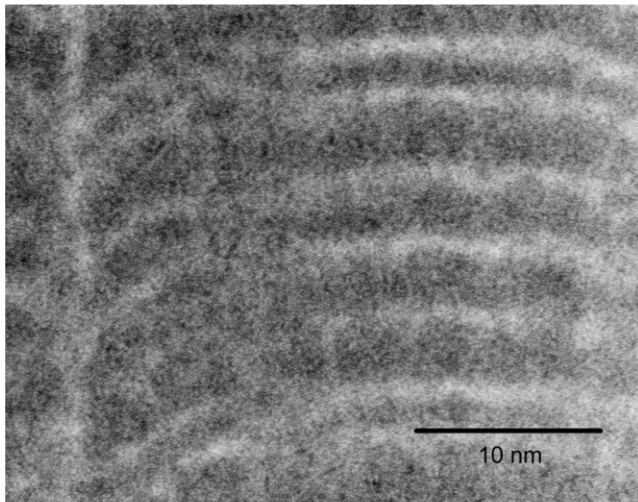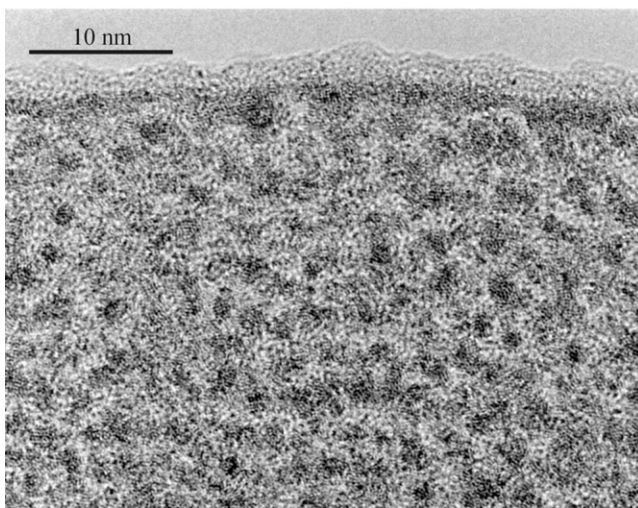
Fig. 6. Overview with cross-section TEM from (a) 25 sccm and (b) 140 sccm acetylene flow.

WC rich and carbon rich separate layers is clearly visible. The periodicity of the multilayer for the four different coatings were $\lambda = 50.7$ nm for the coating with 25 sccm acetylene, $\lambda = 65.4$ nm for the 50 sccm acetylene, $\lambda = 83$ nm for the 100 sccm acetylene and $\lambda = 104$ nm for the 140 sccm acetylene. The origin of the multilayer is from the substrate table rotation (one-fold) when the test pieces are moving in and out of the WC target area. When the test pieces are passing the target area, metal rich Me-DLC is deposited and outside the target area, carbon rich coating is deposited. This means that the period of the multilayer is strongly influenced by the PA-CVD directly from hydrocarbon (acetylene) gas phase. The higher the partial pressure of acetylene, the more contribution of PA-CVD a-C:H. The measured trend in the multilayer period from the investigated W-C:H coatings, with the 25 sccm acetylene flow having the shortest period and the 140 sccm the longest period, verifies this clearly. All the coatings have a columnar structure. Details of the multilayered structure for the coatings with 25 and 140 sccm acetylene were also studied in high resolution cross-section TEM (Fig. 6a,b). The darker ribbons in the micrographs represent WC rich layers and the brighter bands represent carbon rich layers within the multilayered coating structure. It can now be observed that there is a multilayer structure of higher spatial resolution present in the coatings, than could be detected with SEM. The periodicity varies between roughly 5 and 15 nm. This variation in the multilayer period is a result from the two-fold planetary rotation of the substrate table, when the spindle with the test pieces itself is rotating around its axis. Because of the gearing ratio in the substrate table, the twofold rotation is faster than the onefold substrate rotation, thus resulting in a multilayer structure with a higher spatial resolution. The coating with 140 sccm acetylene is in general brighter than the coating with 25 sccm acetylene, indicating that the carbon content is higher. There are no indication of uniformly dispersed nano-WC crystallites in the WC rich layers, like discovered in previous work [11] with W-C:H layers deposited with W targets. The distribution of WC in the WC rich layers, in the case of W-C:H deposited with WC targets, is more like areas or ribbons, rather than uniformly dispersed 2–3 nm sized WC crystallites like in previous work, see Fig. 7a,b. The reason for this behavior is not yet fully understood and will be subject to further investigation.

- By using a low flow of acetylene, a very hard W-C:H coating could be deposited. With a higher flow of acetylene, the W-C:H coating became softer. The hardness of the W-C:H coatings could be varied between 8 and 27.5 GPa.
- The stress measurement showed that the stress level in the W-C:H coatings was lowered with a higher flow of acetylene.
- Investigation of the microstructure of the W-C:H coating by cross-section SEM showed that the coatings have a pronounced multilayered structure with a λ between 50.7 and 104 nm, depending on acetylene flow.
- With cross-section TEM, a finer multilayered structure of the coatings could be observed. The multilayer period varied between 5 and 15 nm.
- With high resolution cross-section TEM it was observed that the WC was distributed homogeneously in WC rich layers, rather than uniformly dispersed 2–3 nm sized WC crystallites.

Acknowledgments

References

[1] C.-P. Klages, R. Memming, Mater. Sci. For. 52/53 (1989) 609.
[2] G. Gille, B. Rau, Thin Solid Films 120 (1984) 109.
[3] E. Bergmann, J. Vogel, J. Vac. Sci. Technol. A5 (1987) 70.
[4] M. Murakawa, et al., Surf. Coat. Technol. (1999) 646.
[5] O. Hurasky-Schönwerth, Technical report, Environmentally compatible tribo-systems in gearing, Chair of machine tools-gear research group, Aachen University of Technology (RWTH), 1999.
[6] J. Güttler, J. Reschke, Surf. Coat. Technol. 60 (1993) 531.
[7] D. Roth, B. Rau, S. Roth, J. Mai, K.-H. Dittrich, Surf. Coat. Technol. 74/75 (1995) 637.
[8] W.D. Nix, Metallur. Trans. A 20A (1989) 2217.
[9] D.S. Gardner, P.A. Finn, J. Appl. Phys. 67 (1990) 1831.
[10] K. Bewilogua, C.V. Cooper, C. Specht, J. Schröder, R. Wittorf, M. Grischke, Surf. Coat. Technol. 127 (2000) 222.
[11] C. Strondl, G.J. van der Kolk, T. Hurkmans, et al., Surf. Coat. Technol. 142–144 (2001) 707.

Fig. 7. High resolution cross-section TEM images with comparison of WC crystallite formation of W-C:H coatings made with (a) WC targets and (b) W targets.

4. Conclusions

- The coefficient of friction was significantly lowered by incorporating more a-C:H into the W-C:H coatings by using a higher flow of acetylene during the deposition process. The coefficient of friction could be varied between 0.129 and 0.312 under dry sliding conditions.